Journal homepage www.jzs.univsul.edu.iq
Journal of Zankoy Sulaimani
Part-A- (Pure and Applied Sciences)

Evaluation of tension stiffening and moment-curvature of high performance reinforced concrete beams under sustained load

Kawa Taha Abualwafa Ahmed
Faculty of Civil Engineering -Sulaimani University, Bakrajo Street, Sulaimaniyah
E-mail: kawaa54@yahoo.com.

Article info
Original:08.07.2015
Revised:14.12.2015
Accepted:28.01.2016
Published online:
20.06.2016

Key words: *Sustained Load, High performance reinforced concrete, Eurocode2, MC 90, Tension*

Abstract

In this paper, the effects of creep and shrinkage on the deflection and cracking of reinforced high performance concrete beams subjected to sustained load type in bending are investigated. Mid-span deflections, cracking and surface strain profiles were monitored over a 90 day period so that to verify the structural response of HPRC (high performance reinforced concrete) beams. Using the results obtained from the experiments, the effect on tension stiffening was examined. Four concrete strengths 52, 95, 96 and 100 MPa were included as a major experimental parameter. The results showed that as higher strength concrete was employed, not only cracks along the reinforcement more extensive, but also the transverse crack spacing became smaller. Thereby, the effective tensile stiffness of the high-performance concrete specimens at the stabilized cracking stage was much smaller than those of normal-strength concrete specimens. This observation is contrary to the current design provisions, and the reduction in the tension stiffening effect by employment of high-performance concrete is much greater than that would be expected. Measured surface strains in both the tension and compression zones of beams of HPC subjected to sustained load were considerably higher than the normal strength concrete beam. This was thought to be primarily due to the effects of creep in the compression zone and a higher degree of cracking within the tension zone. The progressive long-term increase in deflection is shown to be a result of strain development primarily in the compression zone. The sustained load is shown to affect the section stiffness most significantly within the early stages of loading. Using experimental results, the validity of Eurocode 2 (EC2) is examined.

1. Introduction

In the past, high-performance concrete (HPC) has been successfully used in the design of reinforced concrete columns. However, more recently there is evidence that it is becoming increasing popular to use this material in spanning elements; concrete with a compressive strength in excess of 100 MPa will inevitably lead to smaller member depths, which is seen as a positive. The corollary of this, however, is that this may also lead to higher stresses in the tension steel reinforcement.

Whilst the Ultimate Limit State (ULS) performance of these spanning elements under short term loading is easier to understand and quantify (and in many ways can be considered an extension of the ULS performance of normal strength concrete (NSC) spanning elements), the serviceability performance of this 'new' composite (in particular long-term deflection and cracking) is less certain. There are 3 main components which contribute to the long-term deflection of cracked reinforced concrete elements; these are shrinkage, creep and loss of tension stiffening (in the design codes, the latter two are normally considered together); all three contribute to the complicated redistribution of stresses between the steel and the concrete which occur time-dependently within the structural section. The question is whether the behaviour of this high performance concrete can be predicted using theory which was originally developed from NSC– in particular for this paper, is the loss of tension stiffening comparable with that witnessed in NSC spanning elements?

Predominantly, reinforced concrete members are designed to crack. Once cracked, the stiffness of the element as a whole are reduced; this reduction in stiffness depends on the degree of cracking and how close the element is in a stabilized crack pattern. The maximum reduction in stiffness will be at a crack where the compressive forces are only assumed to be balanced by the tension force in the steel (in order to achieve equilibrium); assuming a stabilized crack pattern, midway between two cracks in the stiffness will be unchanged (assuming no internal cracking has propagated to this midpoint region) as the concrete below the neutral axis still contributes. Thus the concrete between the cracks contributes to the stiffness of the tension member, and this effect is normally called the tension stiffening effect [1 and 2]. Such a tension stiffening influence in a flexural member is not quite the same as that in an axial member because the tensile stresses in a cracked flexural member are induced not only by the steel reinforcement–concrete bond but also by the curvature of the flexural member [3]. This tension stiffening effect that arises from the ability of the concrete to carry tension between cracks in an RC member helps control member stiffness, deformation, and crack widths all of which are related to satisfying serviceability requirements [1]. For NSC, several variables such as the percentage and distribution of reinforcing steel, bar size, bond properties, and shrinkage of concrete have been shown to have an effect on tension stiffening [1]. An experimental study showed an important decay in the tension stiffness due to splitting cracks (secondary internal cracking) along the reinforcement, and they proposed that the effect of tension stiffening should not be taken into account unless the cover to bar diameter ratio c/d_b is more than 2.5 [4]. The tension stiffening effect is highly dependent on the cover thickness and the concrete strength. By increasing the concrete strength, the tension stiffening effect reduced when the c/d_b range reduced below 2.5 (i.e. the loss of tension stiffening was greater than the 0.5 quoted for NSC [2, 5]. Higher strength concrete (HSC) was employed, not only did the peak bond stress become higher, but it also becomes more concentrated near the loaded end [6]. A numerical study found that the tension stiffness of HPC is lower than that of NSC [3]. This was thought to be because HSC is generally more brittle than NSC, and in turn, less stress redistribution can take place at the ultimate loading stage.

Apart from the research cited above, very little other information is available in the literature concerning the time-dependent development of flexural cracking and the effect of long-term behaviour on the tension stiffening decay of high performance reinforced flexural members.

In this study an experimental programme was performed to evaluate the loss of tension stiffness of high performance reinforced concrete beams under sustained load and compare this behavior with that seen in NSC beam.

2. Presence of tension stiffening in the codes

2.1 Predicting long-term curvature

Formulae exist within current design codes which can in theory be used to predict the serviceability behavior (crack characteristics, deflection, etc.) of reinforced concrete flexural members. Within these factors are recommended factors to account for the loss of tension stiffening. As mentioned above tension stiffening reduces under sustained loading due to time-dependent cracking. After the formation of a primary crack, internal cracks are formed at the steel–concrete interface, however, shrinkage-induced degradation of the bond

at the concrete-reinforcement interface and tensile creep between the cracks in the tensile concrete also contribute to its loss [7].

The internal cracks first form along portions of the reinforcement which are adjacent to the primary crack. As adhesion along the bar is lost and stress is transferred to the bar's ribs, internal cracks propagate from the ribs. Internal cracking effectively deteriorates the bond, separating the reinforcement and the concrete. This means that along parts of the reinforcement where internal cracking has occurred, the two materials cannot behave in a composite manner and the tensile force is not effectively transferred from the steel to the surrounding concrete. Because of this, internal cracks lead to further loss of section stiffness and also higher average stresses in the deboned steel. Experimental investigation was carried out on axially loaded RC specimens [7]. However, it is commonly acknowledged that in an RC member subjected to a bending moment, the tension steel and surrounding concrete behave similarly to the axially loaded case. Consequently, internal cracking would also be expected to take place at the steel–concrete interface within the tension region of an RC beam subjected to a bending moment. Furthermore, loading causes continued stress transferral and further internal cracks form at ribs progressively more distant from the main crack. It is generally believed that tension stiffening reduces rapidly after first loading and reduces to about half its instantaneous value within 30 days of loading (provided the stabilized crack pattern is reached) [8, 9 and 10]. The decay of tension stiffening with increasing load is mainly attributed to the formation of new primary cracks during the crack formation phase and due to degradation of bonds during the crack stabilization phase. The formation of each new primary crack causes a loss of concrete tensile stress in the regions adjacent to the crack. After all, the primary cracks have developed, the crack stabilization phase begins. Cover-controlled cracks occur under increasing load at the steel, concrete interface causing a loss of bond and hence a loss of tension stiffening.

The Eurocode 2 [12] approach is adopted for predicting long-term deflections, and the loss of tension stiffening with time. Curvatures increase with time in reinforced concrete flexural members due to the combined effects of creep, shrinkage and loss of tension stiffening. In Eurocode 2, [12] the mean curvature in cracked members is given by

$$1/r_m = (1-\xi)\,1/r_{uncr} + \xi\,1/r_{cr} \quad (1)$$

where

$$\xi = 1 - \beta(M_{cr}/M)^2 \quad (2)$$

where ξ is a distribution coefficient accounting for moment level and degree of cracking.

$1/r_{cr}$ and $1/r_{uncr}$ are the curvatures of the cracked and uncracked sections of the element, respectively; M_{cr} is the cracking moment. The coefficient ξ in equation (2) takes account of loss of tension stiffening with time owing to additional internal and macro-cracking under sustained load. Eurocode 2 [12] states that β should be taken as 1 for short-term loading and 0.5 for long-term loading, but does not define the variation in β with time.

The experimental work carried out a series of relatively short-term tests (up to around 100 days) on tension members which showed that the residual tensile force resisted by cracked concrete reduces to its long term value within a few weeks of loading. The specimens were first loaded around 28 days after casting. They found that the long-term mean residual tensile stress in the concrete between cracks was around half the instantaneous value after first cracking. The tension stiffening was largely lost owing to additional cracking and internal damage under sustained load as the tensile strength of concrete reduces to around 70% of its instantaneous value under sustained loading. The time function describing the rate of loss of tension stiffening in tension specimens is approximately

$$\beta(t) = -0.12\log_{10}(t) + 0.65 \text{ with } 0.5 < \beta(t) < 1.0 \quad (3)$$

where $\beta(t)$ is a function of time and t is the time in days from first cracking. The tension stiffening is lost rapidly in slabs, but at a slower rate than in tension specimens. The β value should be taken as 0.5 in most cases in Eq. (2) [13]. Also the β value typically reduced from 1 to around 0.7, in cracked members, between

1 and 2 days after first loading [14]. The creep and shrinkage strains were typically determined from control specimens which had a significantly smaller notional size v/s ratio than the slabs. It was therefore difficult to accurately assess the contributions of creep and shrinkage to a deflection in the first few days after loading [14].

2.2 *Crack width formula (flexural elements)*

Eurocode 2 [12] gives the following expression for the mean tensile strain $(\varepsilon_{sm} - \varepsilon_{cm})$ as follows:

$$(\varepsilon_{sm} - \varepsilon_{cm}) = \frac{\left(\sigma_s - k_t\left(\frac{f_{cteff}\left(1+\alpha_s\rho_{eff}\right)}{\rho_{eff}}\right)\right)}{E_s} \geq 0.6\frac{\sigma_s}{E_s} \quad (4)$$

where k_t is the factor expressing the duration of loading: k_t= 0.6 for short term loading and k_t= 0.4 for long term loading, σ_s is the stress in the tension reinforcement calculated on the basis of a cracked section, α_s is the modular ratio $\frac{E_s}{E_c}$, and f_{cteff} is the mean value of tensile strength of the concrete, effective at the time when the cracks may first be predicted to occur,

$$\rho_{eff} = \frac{A_s}{A_{ceff}} \quad (5)$$

A_{ceff} = effective tension area, is the area of concrete surrounding the tension reinforcement.

The term $\frac{\left(k_t\left(\frac{f_{cteff}\left(1+n\rho_{eff}\right)}{\rho_{eff}}\right)\right)}{E_s}$ represents the tension stiffening amount.

2.3 *Crack width formula (axial elements)*

According to the design code for tension stiffening of tension members in MC 90 (CEB-FIB model code 1990) [1], the overall tension stiffening behaviour is expressed in terms of the mean steel strainε_{sm}. The average strain in the reinforcement in the stabilized cracking stage is given by

$$\varepsilon_{sm} = \varepsilon_{s0} - \beta\frac{f_{ct}}{E_s\rho} \quad (6)$$

where ε_{s0} is the strain in tension reinforcement at the cracked section, β is an experimental constant accounting for the effects of tension stiffening with 0.40 for short term loading, and 0.25 for long-term or repeated loading, f_{ct} is the tensile strength of concrete, E_s is the modulus of elasticity of steel, and ρ is the ratio of reinforcement.

3. Experimental Details

3.1. Details of materials and specimens

Table 1 gives details of the concrete mix proportions used for this investigation. Three HS mixes and one NS mix were used to cast 4 beams. The properties of the mixes are shown in Table 2. The compressive and flexural strength of the concrete was measured on companion specimens (in the form of concrete cubes 100 mm x 100 mm x 100 mm and prisms 100 mm x 100 mm x 500 mm) at various times. Correspondingly, the creep and shrinkage strains were measured on separate specimens with dimensions of 75 mm × 265 mm (diameter × length). Creep tests in compression for each batch of concrete were carried out using standard creep rigs, each containing two 75 mm diameter cylinders loaded with a constant sustained load of 20% of the ultimate compressive strength applied at age 14 and 28 days. The creep strain was determined by subtracting the measured shrinkage strain and the instantaneous elastic strain from the total strain measured on the creep cylinders. The creep coefficient at any time was determined as the measured creep strain at that time divided by the measured instantaneous elastic strain. The concrete was stored under two different

conditions, environments, for a period of 14 and 28 days, in order to know how the age of concrete (i.e. strength) affects the creep and shrinkage of concrete in two different ages. The measured creep coefficient for concrete loaded at age 14 and 28 days and shrinkage strain is presented in Figs. 1 and 2.

Table 1: Details of Mix proportion contain different levels of Silica Fume for beams B1H, B2H, B3H and B4M

Mix	SF (%)	SP (%)	W/B Ratio	Weight of ingredients Kg/m^3					
				W	C	S.F	CA	FA	SP
1	0	0.0	0.55	184	311	0	1249	633	0.0
2	5	0.8	0.28	137	441	23	1070	773	10.0
3	15	1.0	0.25	135	442	78	1070	709	11.0

Table 2: Material Properties for High Performance and Normal Strength Concrete

Specimens	Mix	Concrete compressive strength ($f_{ck,cube}$) (MPa)	Concrete flexural tensile strength (MR) from experiment ($f_{ct,fl}$) (MPa)				Concrete Flexural tensile strength (MR) using EC2 (f_{ctm}) (MPa)	
		14 d	28 d	14 d	28 d		14 d	28 d
B1H	2	88.17	95.05	6.7	11.2		4.83	5.65
B2H	3	97.16	100.0	10.4	11.4		5.00	5.67
B3H	3	92.97	96.42	-	11.3		4.70	5.43
B4N	1	48.93	52.26	-	5.5		3.46	3.61

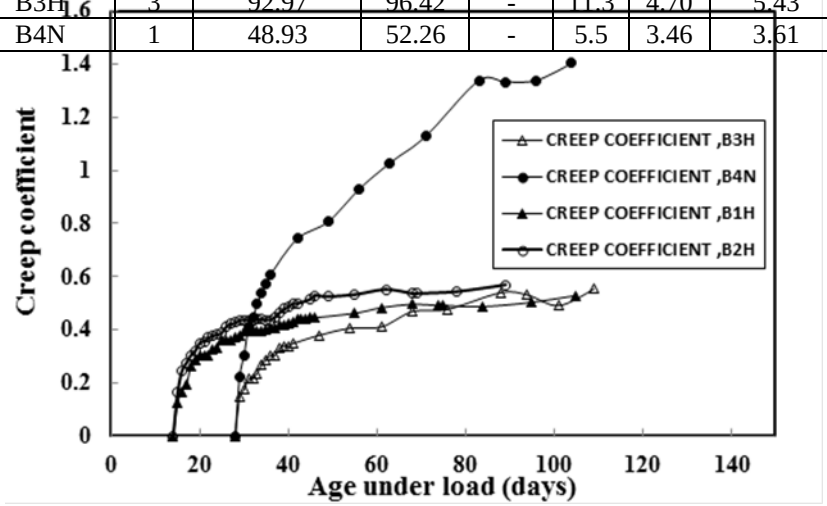

Figure 1: Creep coefficient for concrete with age

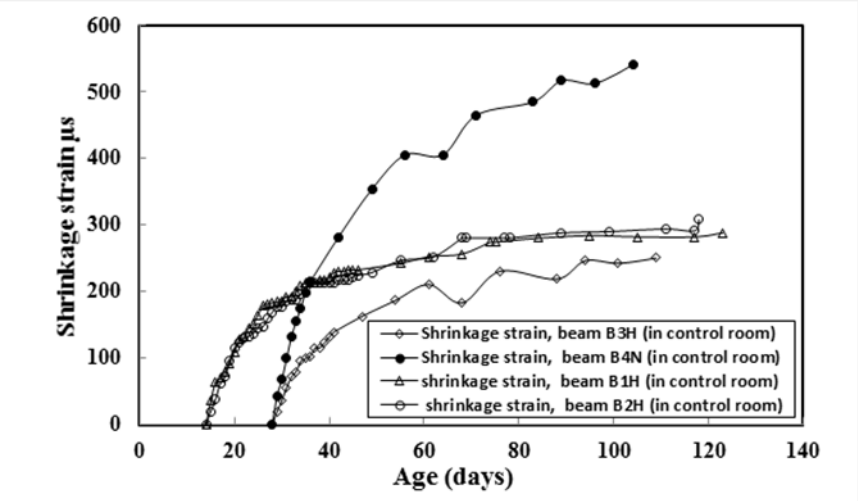

Figure 2: Shrinkage strain for concrete with age

3.2 *Details of beams*

To minimize the shrinkage during the curing procedure, wet curing was provided for 3 days after concrete casting until demoulding, and afterwards transferred to a fog room (relative humidity 100 % and temperature 21 ± 1^0C) for a period of 14 and 28 days, in order to know how the creep of concrete affect the deflection in two different ages. After 14 and 28 days, the beams were removed from the fog room and placed in the test rigs (the ambient temperature is in the range of 20–25◦C and the relative humidity is between 40 and 60 percent). The concrete was stored under two different conditions, environments for a period of 14 days for beams 1H and 2H and 28 days for beams 3H and 4N, in order to know how the creep of concrete effects the deflection in two different ages. In order to monitor the depth of neutral axis /curvature with time, the strain developments are the profile for each beam and they are measured from the Demec gauges (200 mm) were used to measure the horizontal strain on the side of the beam in the region of the constant moment zone. Eight sections from both faces of beams were considered in the analysis of surface strains of concrete. These sections were located at a distance of 200 mm from the centre of the beam and at different levels. The strain was measured at four different depths, two of which at a level which was equal to the tensile reinforcement level, at a level 25 mm below the top of the beam (i.e. in the compression zone), and the other at 28 mm centre to centre between top and bottom level.

Linear Variable Displacement Transducers (LVDTS) were attached to the soffit of each specimen at five positions, three of them in the constant moment zone and the other at both supports, to measure deflection at the middle and supports of each specimen. All beams were 4200 mm long (clear span 4000 mm), 150 mm deep and 300 mm wide; the constant moment zone was 1500 mm. Three ∅16 mm bars were used as bottom longitudinal tension reinforcement. Shear links (∅ 8 mm at 125 mm$^{c}/_{c}$) where used, however, as the beams were tested under a traditional 4-point bending test arrangement, the links were not placed in the constant moment zone. The cover to the shear links was set at 20 mm. Fig. 3 shows the geometry and instrumentation for a typical test beam.

The load was incrementally applied and maintained for three months to observe the time-dependent behavior. The beams were subjected to loads which in theory only slightly exceeded the cracking moment – the intention was not to monitor beams with a stabilized cracking pattern, but to observe any development in cracking due to the time-dependent load. The time-dependent deformations were measured every day for the first week then every seven days. To measure the steel strains in the critical moment regions (e.g. constant moment zones), one electric resistance strain gauge was attached to each of the main reinforcement bars. The strain gauges were connected to an HBM amplifier. Finally, a microscope with a magnification factor of 40 was utilized to measure the crack widths.

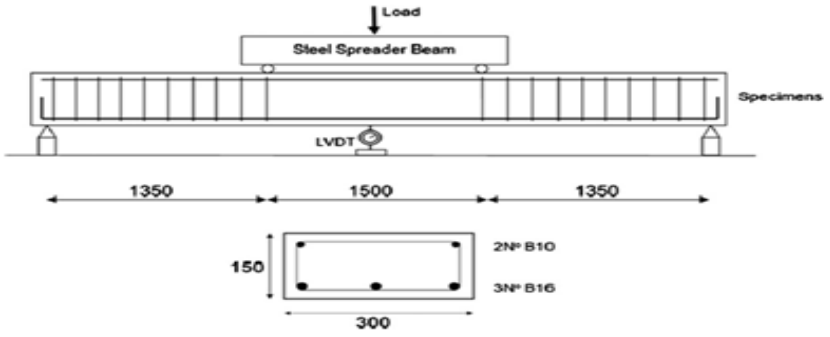

Figure 3: Beam dimension, reinforcement and experimental set-up

4. *Mid-Span Deflections*

Investigation results for mid-span beams deflections are shown in Fig. 4 for all beams tested under a sustained load (beams B1H, B2H, B3H and B4N), showed that deflection at mid-span increases rapidly over the first 1-2 months after loading with more than 60% of the final deflection occurring within this period for beams. This rapid increase in deflection caused by the loss of stiffness due to the development of time-dependent cracking and the increase in deformation caused by creep and shrinkage and loss of tension stiffening. The rate of change gradually decreases for the remaining part of the test. This would suggest that actions within the early stages of loading create the discrepancy between the deflections of beams under the sustained load, but after this initial period, the difference between deflections remains approximately variable. As all measurements were taken at the different load level, the additional loss of stiffness, hence the additional deflection can be said to be a result of previous loading as shown in Fig. 4.

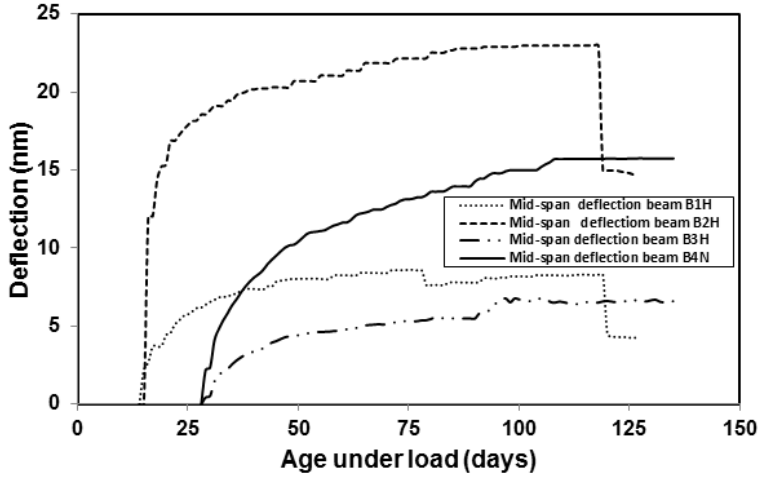

Figure 4: Measured mid-span beam deflection vs. age under load

Moreover, in order to compare the behaviour of all beams regarding the creep, shrinkage and deflection the ratio of shrinkage, creep and deflection for beams B1H, B2H, B3H and B4N are presented in Table 3. It is observed that the measured long-term deflections for beams B1H, B2H and B4N are greater than that of B3H. This may be due to the high compressive strength and modulus of elasticity at the age 28 days. In addition to this, shrinkage strain, creep and creep coefficient for B3H are lower than those for the other beams. The measured long-term deflections for beams B3H and B4N at age 90 days are 6.60 mm and 15.74 mm, respectively, which are 12.20 and 7.16 times the corresponding instantaneous deflections, respectively. At

the end of the testing period of three months, the load was removed from beams B1H and B2H and the rate of deflection recovery was monitored. Ninety percent recovery of the deformation occurred instantaneously, while the rest was achieved after seven days of the load removal. Therefore, it can be concluded that the amount of long-term deflection due to creep and shrinkage was 7.44, 10.97, 6.06 and 13.55 mm for beams B1H, B2H, B3H and B4N, respectively, that caused due to the condition of the beams immediately after loading and under the effect of sustained load.

On average, the HPC reinforced concrete beam B2H under the sustained load of 12 kN showed deflection due to creep and shrinkage about 33% greater than that of beam B4N under sustained load of 4.3 kN, and about 58 and 70% greater than that of beams B1H and B3H, respectively under the similar sustained load of 8 kN. The measured final long-term deflection also, compared to the long-term deflection predicted using the EC2 approach as summarized in Table 4. The results showed that there were the large differences between the two in relation to the impact of shrinkage and creep and loss of tension stiffening. In addition to this, it was found that the measured deflections for the duration of 90 days lower compared to the values predicted by the EC2. The differences are borne out of all the pertinent parameters, namely: the properties of mortar, modulus of rupture, modulus of elasticity, sustained loads, creep and shrinkage. In addition to these, the reason being using high-performance concrete for beams increased their flexural rigidity and reduced immediate and long-term deflections. Alternatively, the cause may be due the reduction of the water to binder ratio resulted in a substantial increase in compressive strength of concrete and because of this, their flexural rigidity increased. The prediction of long-term deflection looks reasonable for the NSC, but grossly over-predicts for the HSC. B2H prediction is closer this is because there is a more elastic deflection in the experiment and predicted values.

Furthermore, Table 4 compares the predicted long term Mid- Span deflection using EC2 with different values for beta. It can be seen that the NSC beam with a beta value of 0.74 would make the prediction of deflection more accurate.

Additionally, it was concluded that if the same analysis was performed for calculating the long-term deflection using EC2 approach. But, for calculating the cracking moment, $M_{cr,}$ the flexural tensile strength (Modulus of rupture) is used instead of the tensile strength directly from the EC2 equations, the results for the final long term deflections were found to be lower than the final long term deflection using the tensile strength from the EC2 equation for computing the cracking moment M_{cr}, i.e. theoretically. Because, in this investigation the flexural tensile strength using flexural test method was performed for beams and it was found that the flexural tensile strength for HPC higher than the tensile strength using the EC2 equations. This is usually attributed to the dense microstructure which develops in the mature system, which is the result of the small size of the silica fume particles that pack between the cement grains, and their relatively quick pozzolanic reaction. While the improved transition zone and enhanced matrix-aggregate bond, which could be translated into higher strength, could limit particle or solid movement, which is associated with long-term creep [15].

The NSC the reduction in stress is likely related to tensile creep, shrinkage restraint and increased cracking over time, as well as possibly degradation of bond of the reinforcement near the cracks. Furthermore, the long-term loading, the tension stiffening value reduces to approximately half its initial value [2].

Table 3: Ratio of shrinkage, creep and deflection for beams 1, 2, 3 and 4

B1H AND B3H			**B2H AND B3H**			**B4N AND B3H**			**B1H AND B4N**		
SB1/ SB3	**CB1/ CB3**	**DB1 /DB3**	**SB2 /SB3**	**CB2 /CB3**	**DB2 /DB3**	**SB4 /SB3**	**CB4 /CB3**	**DB4 /DB3**	**SB4 /SB1**	**CB4 /CB1**	**DB4 /DB1**
1.06	0.484	1.52	1.14	0.63	4.43	2.09	0.95	2.94	1.97	1.95	1.92

Table 4: Load, Deflection for Beams B1H, B2H, B3H and B4N

Specimen	Sustained load at first crack (kN)	M_s (kN. m)	Long-term deflection (Experiment) (mm)	Long Term Mid- Span Deflection Using EC2 (mm)		
				β=0.5	β=1	β=0.74
B1H (HPC)	8.0	8.63	9.66	23.64	15.64	19.80
B2H (HPC)	12.0	11.25	23.0	29.12	17.28	23.43
B3H (HPC)	8.2	8.75	6.70	27.63	15.78	21.94
B4N (NSC)	4.3	6.31	15.75	25.64	15.79	20.92

5. Crack width and spacing

Figs. 5 and 6 show the development, range, and width of cracks within the high moment regions was observed immediately after first loading and during the test period (90 days). Test results show that the beam specimens, the maximum crack width within the high moment region increased rapidly in the first few weeks of loading when the creep and shrinkage strain developed rapidly. Further to this, the results show that average crack spacing changes with time and further cracks developed under sustained loads between widely spaced cracks within the primary stabilized crack pattern (mainly due to shrinkage), and the final average crack spacing consequently reduces. The final maximum crack spacing for B1H and B2H is only about *0.9 and 0.6 of* the instantaneous value, respectively. The ratio for instantaneous to final crack width was 0.1 for B1H and 0.16 for B2H, respectively. While this ratio for instantaneous to final crack width was 0.94 for B3H and 0.32 for B4N. In addition to this, the length (height) and width of cracks was also noted to increase with time, mainly due to shrinkage, and the final average crack spacing consequently decreases. Furthermore, the length of some of them reached almost half depth of the beam. In the long-term tests where the load was maintained constant after cracking of the member, the experimental results show that the contribution of the tensile concrete decreases with time.

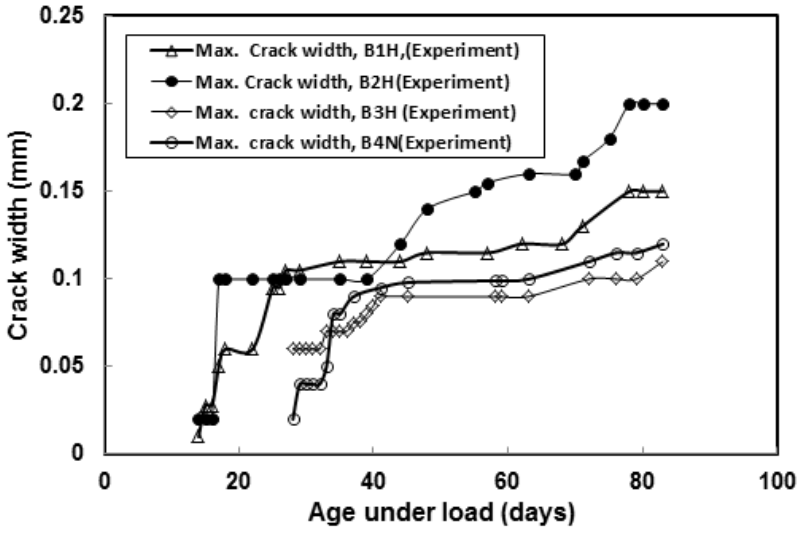

Figure 5: Development of crack width vs. age under load

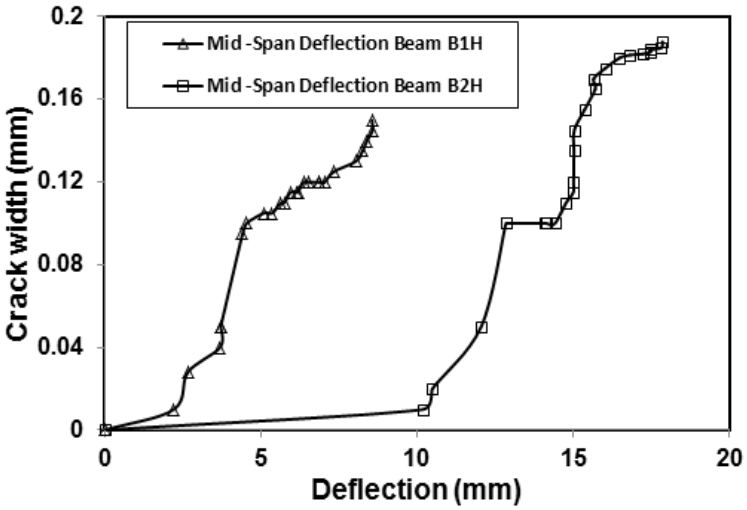

Fig. 6: Relationship between crack width and mid-span deflection

6. Tensile and compressive strain development

Fig. 7 shows the surface strain development within (a) the beam's compression zone (measurements taken 25 mm from the top of the beam) and (b) the beam's tension zone (measurements taken at the tensile reinforcement level) with respect to time under load. Top fibre concrete strain at different levels obtained by averaging strain readings along each section at different levels at constant moment zone. The strain values presented here are the total measured strains less the strains measured immediately after the beams were preloaded with 8.00, 12.00, 8.20, and 4.30 kN (i.e. the strain development after initial loading). Presenting data in this way better illustrate the rate of strain increase with time. Initial measured strains are presented within the strain profiles shown in Figs. 10 and 11. Compression and tension strain continually changed with time in order to keep the balance between them and during these changes the position of neutral axis also, went up or went down to remain this balance during the test period under the sustained load. Development of stresses and strains in the reinforcement are shown in Fig. 11 below.

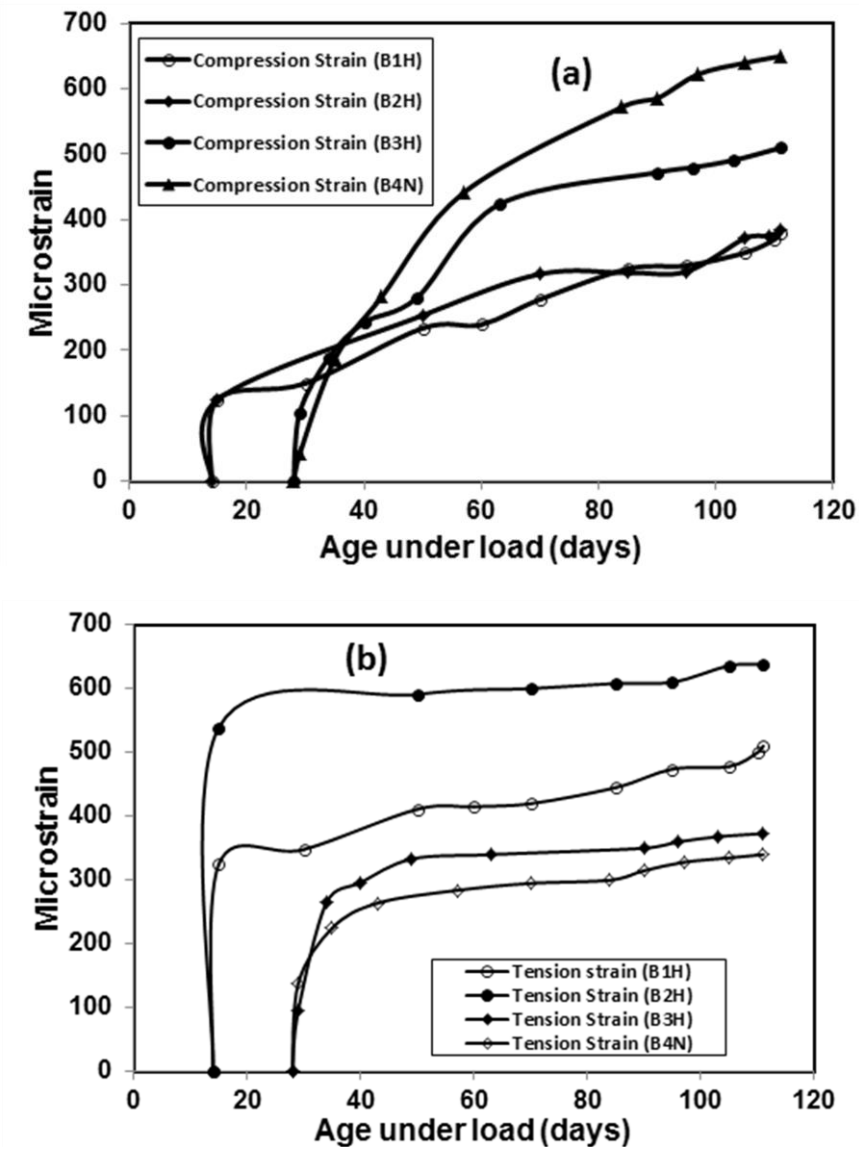

Figure 7: Strain development (discounting initial strain) vs. age under load for (a) compression zone and (b) tension zone at reinforcement level

It was considered that strain recording and interpretation of some interesting information such as strain-moment relationships, moment-curvature relationships and neutral axis position during the testing. Results are presented in Figs. 12 and 13 for strain profile in the concrete. As it could be observed, the compression area seems to increase with the increase in strength. Subsequently, the neutral axis moves down from to the top fibre. The displacement of the neutral axis towards the bottom fibre was recorded to be more evident in all beams due to the same amount of reinforcement ratio. Also from the same figure, one could calculate the curvatures. For example, for B1H the value of the curvature is $13.78 \times 10^{-6}\ mm^{-1}$ while for B2H it slightly reduced to $13.40\times 10^{-6} mm^{-1}$. The decrease in curvature matches the tendency observed on the time-deflection curve, that deflection decreased with the increase in strength. As the moment increases and cracks start to affect the concrete in tension, the position of the neutral plane changes so that equilibrium of forces and moments is maintained.

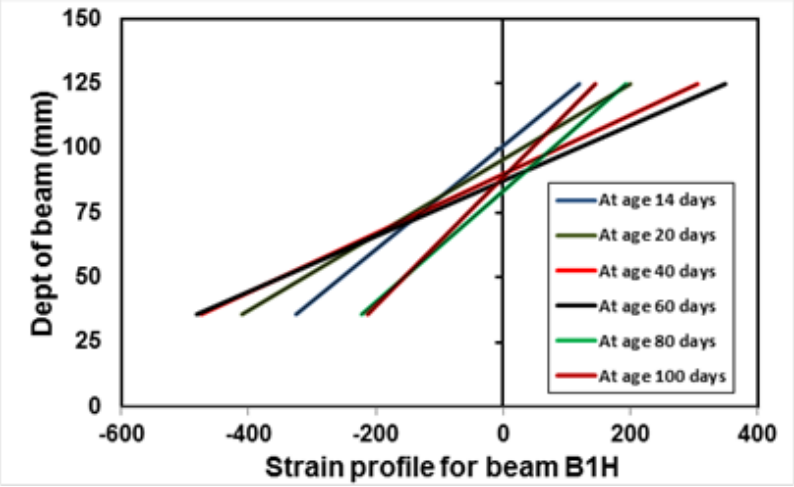

Fig.8: Concrete surface strain at different ages for beam B1H

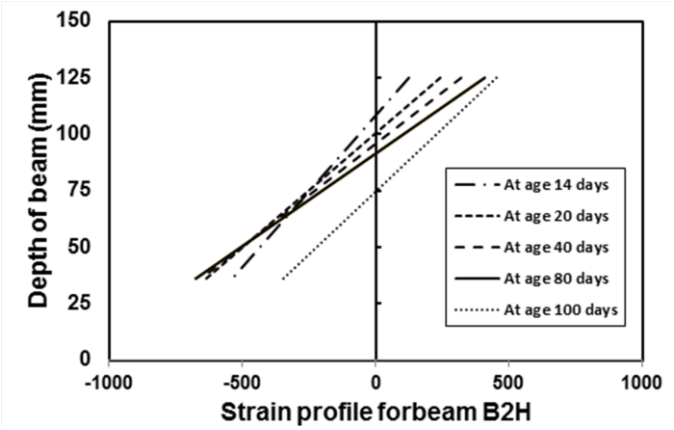

Fig.9: Concrete surface strain at different ages for beam B2H

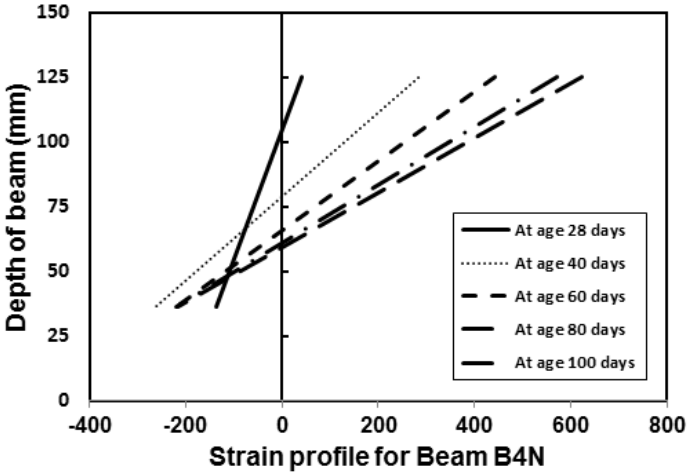

Fig.10: Concrete surface strain at different ages for beam B4N

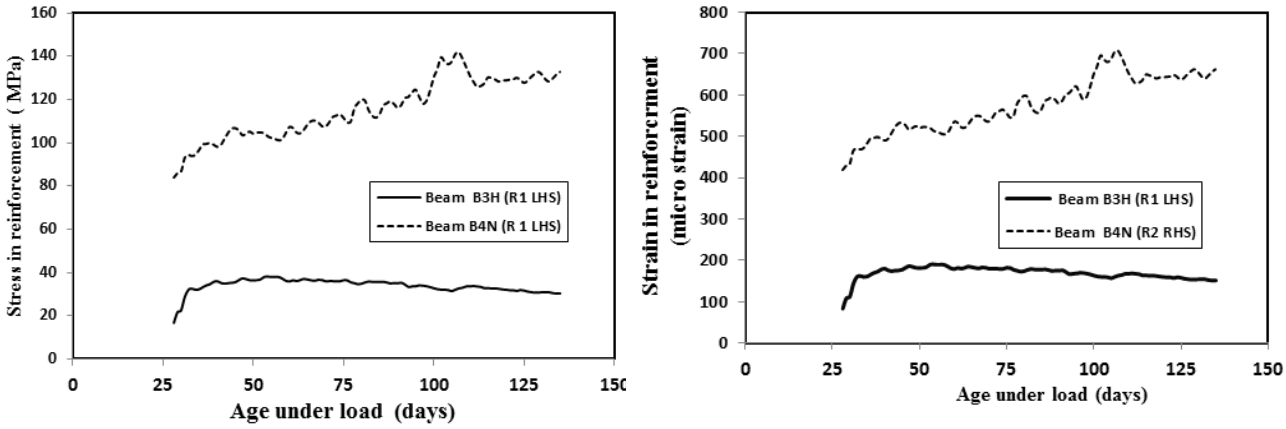

Fig.11: Development of (a) stress and (b) strain in the left hand side (LHS) reinforcement with age.

7. Moment curvature relationship and tension stiffening

Investigation result from the moment curvature relationship, Figs.12 and 13 showed that at the early age of concrete the tension in the concrete between the cracks was high, then continues to reduce during loading after cracking which was not stabilized crack pattern at the applied load, then approximately all the tension stiffening has disappeared by the end of the test. Further, it can be seen that the loss of tension stiffening occurred very rapidly. The reason for the reduction in stress is likely that the main mechanism is not creep. It is well known that modern high performance concretes adopting low water/binder ratio are sensitive to crack at an early age. The driving forces to cracking during concrete hydration are thermal and autogenous deformations. However, the cracking tendency of concrete is determined by many factors such as shrinkage potential, shrinkage rate, tensile strength, Young's modulus, restraint conditions and tensile creep, etc. [16 and 17]. The reduction in tension stiffening is usually attributed to the dense microstructure which, develops in the mature system, which is the result of the small size of the silica fume particles that pack between the cement grains, and their relatively quick pozzolanic reaction. The refined pore structure could restrict the movement of water, which is associated with initial [15]. While the improved transition zone and enhanced matrix-aggregate bond. Furthermore, the hydration and pozzolanic reaction of SF could have used up part of the water, as indicated by higher autogenously shrinkage in the HPC. Higher autogenous shrinkage in the HPC caused more shrinkage restraint. Restraint to shrinkage causes tension that not only reduces the cracking moment and causes time-dependent cracking; it also causes a reduction of tension stiffening with time [18], as a result in the development of more bond micro cracking. Investigation results showed that for the HPC through, the long-term loading, the tension stiffening value reduced to approximately 80% its initial value in the HPC.

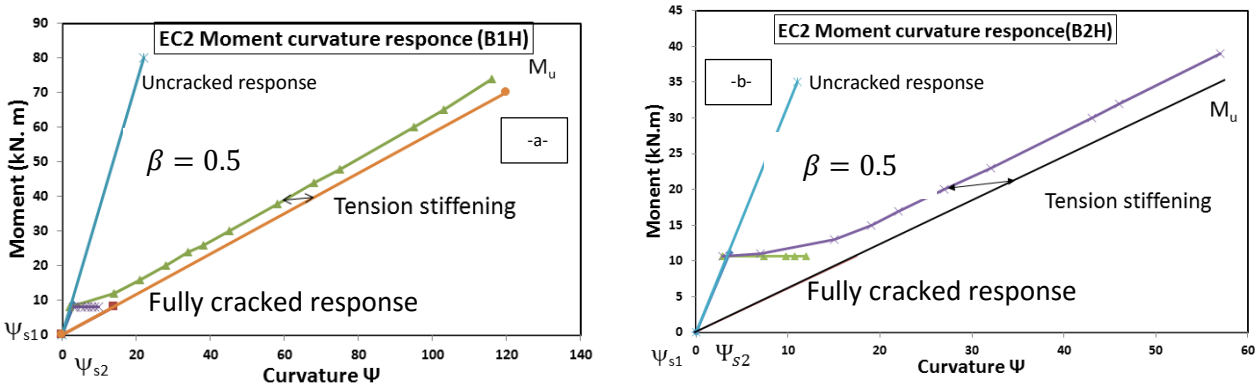

Figure 12: Moment–Curvature relationship for beams at age 14 days of curing (a) B1H and (b) B2H

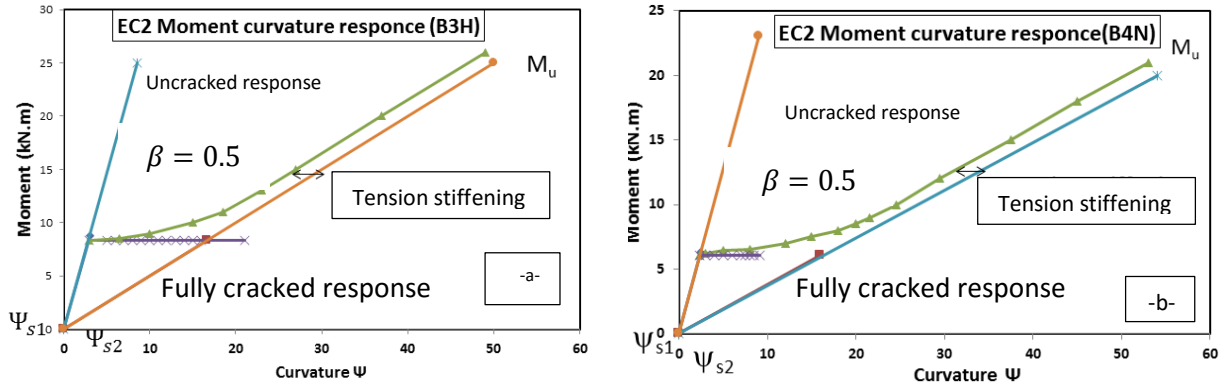

Figure 13: Moment–Curvature relationship for beams at age 28 days of curing (a) B3H and (b) B4N

8. Conclusion

It can be concluded that under sustained load the long-term deflection at mid-span increased rapidly at the early stage of the test within more than 60% of the final deflection occurring within this period for beams. This rapid increase in deflection caused by the decay of tension stiffening due to the progress of time-dependent cracking and the increase in deformation caused by creep and shrinkage and loss of tension stiffening. Then after that, the rate of change gradually decreased in the remaining part of the test.

The maximum crack width within the constant moment region increased rapidly in the first few weeks of loading when the creep and shrinkage strain developed rapidly. The average crack spacing changed with time and further cracks developed under sustained load between widely spaced cracks within the primary stabilized crack pattern (mainly due to shrinkage), and the final average crack spacing consequently reduced. Furthermore, we observed that the tension stiffening effect is highly dependent on the concrete strength. As the concrete strength becomes higher, the tension stiffening effect becomes smaller. This is attributed to it being more probable that splitting cracks along the rebar is coincided with transverse cracks in high performance concrete. The crack spacing between the adjacent transverse cracks, becomes narrower as higher strength concrete is used, a reduction in the crack spacing of 30–50 % as the concrete compressive strength increased. At the early age of concrete the tension in the concrete between the cracks was high, then continued reduced during loading after cracking which was not stabilized crack pattern at the applied load, then approximately all the tension stiffening has disappeared by the end of the test. Through the long term loading, the tension stiffening value for the HPC reduced to approximately 80% its initial value.

References

[1] CEB-FIP. (1991). CEB-FIP Model Code 1990, Comite Euro- International Du Beton, Paris, France.
[2] Beeby, A. & Scott, R. 2006. "Mechanisms of long-term decay of tension stiffening". *Magazine of concrete research.* 58**,** 255-266.
[3] Ng, P., Lam, J. & Kwan, A. 2010. "Tension stiffening in concrete beams". Part 1: FE analysis. Proceedings of the ICE-Structures and Building, 163, 19-28.
[4] Abrishami, H.H. and Mitchell, D. (1996). "Influence of splitting cracks on tension stiffening", ACI Structural Journal, Vol. 93, No. 6, pp. 703–710.
[5]. Lee, Gi-Yeol, and Woo Kim (2009). "Cracking and tension stiffening behavior of high-strength concrete tension members subjected to axial load." Advances in Structural Engineering 12.2: 127-137.
[6] Azizinamini, A., Stark, M., Roller, J.J. and Ghosh, S.K. (1993). "Bond performance of reinforcing bars embedded in high strength concrete", ACI Structural Journal, Vol. 90, No. 5, pp. 554–561.
[7] Hungspreug, S. (1981). "Local bond between a reinforced bar and concrete under high intensity cyclic load", Structural Engineering Report No. 81–6, Cornell University, Ithaca, NY, USA.
[8] Goto, Y (1971). "Cracks formed in concrete around deformed tension bars". ACI Journal, 68, No. 26, 244–251.
[9] Bischoff, P. H. (2001). "Effects of shrinkage on tension stiffening and cracking in reinforced concrete". *Canadian Journal of Civil Engineering,* 28**,** 363-374.
[10] Scott, R. H. & Beeby, A. W. (2005). Long-term tension-stiffening effects in concrete. *ACI structural journal,* 102.
[11] Gilbert RI and Wu HQ (2009). "Time-dependent stiffness of cracked reinforced concrete elements". fib London 09, Concrete: 21st Century Superhero, June, London, UK.
[12] Eurocode 2 (2004): "Design of Concrete Structures – Part 1: General Rules and Rules for Buildings"; The European Standard EN1992-1-1.
[13] Beeby A. W. and Scott R. H., (2004). "|Tension stiffening of concrete, behaviour of tension zones in reinforced concrete including time dependent effects". Supplementary Information. The Concrete Society, Camberley. Technical Report 59.
[14] Vollum R. L (2002). "Influences of shrinkage and construction loading on loss of tension stiffening in slabs". Magazine of Concrete Research, 54, No. 4, 273–282.
[15] Neville, A. M., Dilger, W. H., Brooks, J. J., Neville, A. M. & Neville, A. M. (1983). "*Creep of plain and structural concrete",* Construction Press London.
[16] Hansen W. Pane (March 2002). "Early age creep and stress relaxation of concrete containing blended cements", Materials and Structures 35, 92–96.
[17] Heather T. See, Emmanuel K. Attiogbe, Matthew A. Miltenberger (May–June 2003). "Shrinkage cracking characteristics of concrete using ring specimens", ACI Materials Journal 100 (3) 239–245.
[18] Gilbert, R. I. (2013). "Time-dependent stiffness of cracked reinforced and composite concrete slabs". *Procedia Engineering,* 57**,** 19-34.